

新しい安定条件を用いた後方転倒防止制御法の提案

李 微^{**}, 吳 世訓^{***}, 畠 直輝[†], 堀 洋一^{††}

Prevention of Overturn of Power-Assisted Wheelchair using Novel Stability Condition

Wei LI, Sehoon OH, Naoki HATA and Yoichi HORI

Last 10 years we have been experiencing a constant evolution in the field of power assisted wheelchairs, which allows more flexibility of use for disabled people. However, motor output is quite big, and without proper control, power assisted wheelchair are much easier to fall backward than traditional ones. Hence, in this work, to prevent the overturn, three kinds of stability conditions, including the novel one based on Lagrange Equation has been proposed. They are compared by using experimental data and the best one is adopted. Its validity, as well as practicality, is authenticated by experiments on both horizontal plane and slope.

Key words: stability condition, overturn, power-assisted wheelchair

1. Introduction

A power-assisted wheelchair is lightweight, maneuverable, and simple to transport. It represents an entirely new class of wheelchair, and is studied by several researchers. However, motor output is quite big, and without proper control, power assisted wheelchair is much easier to fall backward than traditional ones. Meanwhile, the dynamics of wheelchair is nonlinear and till now there is no practical technique to prevent the overturn of power-assisted wheelchair.

In this work, after introducing present assist technique [2] as well as the system model, three kinds of dynamical stability criteria on level slope will be given. The 3rd one is deduced from Lagrange Equation. It is more sensitive, much easier for calculation. Experimental results are provided to verify these three kinds of criteria. Later, stability criteria on slope will be analyzed. Finally the experimental data will be given.

2. Power-Assisted Wheelchair System

Large numbers of power-assisted wheelchairs are based on two independently driven rear wheels and two front ones. Batteries and two BLDC motors are used to augment the power applied by the user to one or both pushrims [1].

In this work, the power-assisted wheelchair JWII made by YAMAHA in 1996 (Fig.1), is used. In the following, present assist technique and system model will be introduced.

2.1 Present Assist Technique

The assist force of motor is not just times of human torque. The reason is that if assist force descents to zero right after operator stops, the operator cannot feel been assisted. So, as in [2], low pass filter is used for calculating assist force (Eq.1).



Fig.1 The outlook of power-assisted wheelchair JWII

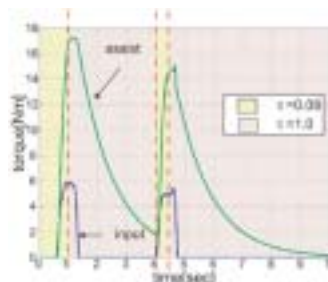


Fig.2 Relationship of Torque Input and Assist

$$T_{assist} = \alpha \frac{1}{1 + \tau s} T_{human} \quad (1)$$

where α is power-assistance-ratio, T_{assist} is the assist force, T_{human} is the input torque from the pushrim, and τ is the time constant. For better ride quality, the ascent should be fast and the descent slow. So in this work time constant τ is decided as the following (Eq.2),

$$\tau = \begin{cases} \tau_{fast} = 0.08[s], & \frac{d}{dt} T_{human} > 0; \\ \tau_{slow} = 1.0[s], & \frac{d}{dt} T_{human} < 0. \end{cases} \quad (2)$$

2.2 System Model

* 原稿受付 2005 年 月 日 .
** 学生会員 東京大学大学院 (東京都目黒駒場 4-6-1) .
*** 学生会員 東京大学大学院 (東京都目黒駒場 4-6-1)
† 学生会員 東京大学大学院 (東京都目黒駒場 4-6-1)
†† 正 会 員 東京大学 (東京都目黒駒場 4-6-1)

When a person is sitting, COM of him and the wheelchair frame is supposed to be at the surface of his abdomen. And by neglecting two front wheels, the model of wheelchair can be represented as Fig.3.

Please note that although two front wheels are not shown in figure, operator cannot fall "forward", and on level ground $\theta_0 > 0$.

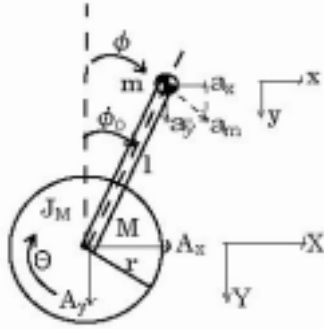


Fig.3 Wheel Model

Table1 Parameters

M	Mass of the driving wheel
m	Mass of operator including wheelchair frame
r	Radius of the driving wheel
J_M	Moment of Inertia of the driving wheel
J_m	Moment of Inertia of operator and frame
	Rotational angle of the driving wheels
	Angle of the vertical to COM
θ_0	Initial angle of the vertical to COM
a_x, a_y	Accelerations of COM
A_x, A_y	Accelerations of the frame

3. Dynamical Criteria of Stability

3.1 Moment Criteria

Assume clockwise moment positive, counterclockwise negative, moment criteria of the system can be written as

$$m(a_y + g)l \sin \varphi - m(A_x - a_x)l \cos \varphi > 0 \quad (3)$$

Usually, when the total moment of system equals 0, system is stable. However, in this work, even when total moment is larger than 0, system is still stable because of two front wheels.

3.2 ZMP (Zero Moment Point) Criteria

The idea of ZMP was introduced by Mr. Vukobratovic at 1969 and 1972 [3]. ZMP is determined by the movement and gravity of the object. As shown Fig.4, the broomstick is influenced by gravitation and inertia force. These combined forces are called the total inertial force. Also, the point where the floor reaction force operates is called the floor reaction point. The intersection of the floor and the axis of the total inertial force have a total inertial force moment of 0, so it is called the Zero Moment Point. It is clear that when ZMP and floor reaction point are the same, system is stable [4].

Fig.5 in [5] shows the simplest case, and by using (Eq.4), ZMP of wheelchair system can be calculated as Eq.5. It is clear that moment criteria (Eq.3) and ZMP criteria (Eq.5) are exactly the same.



Fig.4 Standing a Broomstick Upright

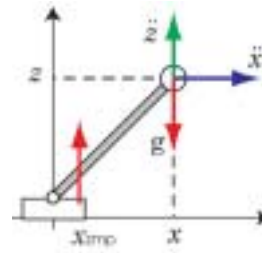


Fig.5 Simple ZMP Calculation Model

$$X_{ZMP} = \frac{\sum_{i=1}^n m_i [x_i (\ddot{z}_i + g) - z_i \ddot{x}_i]}{\sum_{i=1}^n m_i (\ddot{z}_i + g)} \quad (4)$$

$$= \frac{m[l \sin \varphi (a_y + g) - l \cos \varphi a_x]}{m(a_y + g)}$$

$$= l \sin \varphi - \frac{l \cos \varphi}{a_y + g} (A_x - a_x) > 0$$

$$(a_y + g)l \sin \varphi - (A_x - a_x)l \cos \varphi > 0 \quad (5)$$

3.3 Lagrange Criteria

Kinetic energy T of the system model can be calculated as below.

- T = Translational kinetic energy of the driving wheel
- +Rotational kinetic energy of the driving wheel
- +Translational kinetic energy of the body
- +Rotational kinetic energy of the body

The first two items are quite easy to calculate, while the other two are difficult. Assume the velocity of COM is v_G and its horizontal component is v_x while vertical component is v_y . From the Pythagorean theorem, we have

$$v_G^2 = v_x^2 + v_y^2 \quad (6)$$

Meanwhile, v_x, v_y can be calculated by the following equations.

$$\begin{cases} v_{mx} = \frac{d}{dt}(x + l \sin \varphi) \\ v_{my} = \frac{d}{dt}l \cos \varphi \end{cases} \quad (7)$$

Also, the rotational kinetic energy of the body is $J_m \dot{\varphi}^2 / 2$. So the total kinetic energy T is

$$T = \frac{1}{2} M \dot{x}^2 + \frac{1}{2} m v_G^2 + \frac{1}{2} J_M \dot{\theta}^2 + \frac{1}{2} J_m \dot{\varphi}^2 \quad (8)$$

Here, there exists a constraint as

$$r \dot{\theta} = \dot{x} \quad (9)$$

To calculate the potential energy U , we assume that the horizontal plane passing through rear axle as the potential energy reference plane.

$$U = mgl \cos \varphi \quad (10)$$

Now the Lagrangian of the system turns out to be

$$\begin{aligned} L &= T - U \\ &= \frac{1}{2} M \dot{x}^2 + \frac{1}{2} m v_G^2 + \frac{1}{2} J_M \dot{\theta}^2 + \frac{1}{2} J_m \dot{\phi}^2 - mgl \cos \phi \\ &= \frac{1}{2} (M + m) r^2 \dot{\theta}^2 + \frac{1}{2} m l^2 \dot{\phi}^2 + m l r \dot{\theta} \dot{\phi} \cos \phi \\ &\quad + \frac{1}{2} J_M \dot{\theta}^2 + \frac{1}{2} J_m \dot{\phi}^2 - mgl \cos \phi \end{aligned}$$

Equations of motion can be obtained from Lagrange's equations,

$$\begin{aligned} \tau + d\theta &= \frac{d}{dt} \left(\frac{\partial L}{\partial \dot{\theta}} \right) - \frac{\partial L}{\partial \theta} + B_M \dot{\theta} \\ -\tau + d\phi &= \frac{d}{dt} \left(\frac{\partial L}{\partial \dot{\phi}} \right) - \frac{\partial L}{\partial \phi} + B_m \dot{\phi} \end{aligned} \quad (11)$$

Here d and d are disturbances, and $B_M \dot{\theta}$, $B_m \dot{\phi}$ are resistances.

Or more concisely,

$$\begin{aligned} \tau + d\theta &= [(M + m)r^2 + J_M] \ddot{\theta} + m l r \dot{\phi} \cos \phi - m l r \dot{\phi}^2 \sin \phi + B_M \dot{\theta} \\ -\tau + d\phi &= (J_m + m l^2) \ddot{\phi} + m l r \ddot{\theta} \cos \phi - mgl \sin \phi + B_m \dot{\phi} \end{aligned}$$

We simply take into account the wheelchair system model with no wheelie, which means that $\phi = \phi_0$, $\dot{\phi} = 0$, $\ddot{\phi} = 0$, $d\phi = 0$. (The experimental results later will show such simplification is feasible.)

Equation above turns out to be

$$m l r \ddot{\theta} \cos \phi_0 - mgl \sin \phi_0 + \tau = 0 \quad (12)$$

Based on such equation, we calculated with the experimental data, and the results are shown in Fig.6. So it is clear that when

$$\tau < mgl \sin \phi_0 - m l r \ddot{\theta} \cos \phi_0 \quad (13)$$

is satisfied, there is no wheelie and wheelchair system runs safely. Here in this work it is called Lagrange Criteria.

3.4 Remark

It has been stated before that moment criteria and ZMP criteria are essentially the same. On the contrast, Lagrange criteria are much simple, with only two variables, and are much easier to calculate. And in the former 2 criteria, information of accelerations are used meanwhile in the Lagrange criteria, information of torque is used. Acceleration is the result of torque, and as a result Lagrange criteria are much "sensitive" and changes quicker. Also, element "Torque" is included and wheelie can be prevented by regulating it directly.

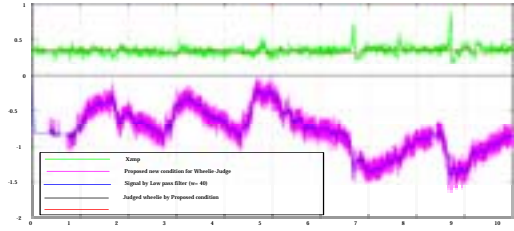
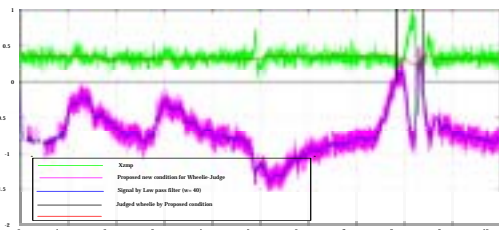
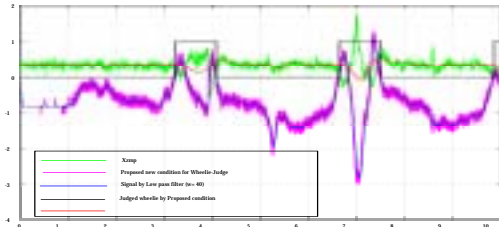


Fig.6 Experiment with 2 times of wheelie, 1 time of wheelie and no wheelie

4. Driving State Observer

Here, an observer that will estimate the inclination angle (ϕ_d) and the driving speed ($\dot{\theta}$) is designed.

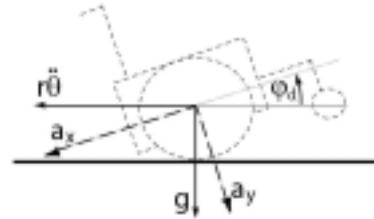


Fig.7 Accelerations Measured by Accelerometer

Here $d_\theta = 0$. And instead of Eq.11, we now take use of the simplified system equations below.

$$J_\theta \ddot{\theta} = -B_\theta \dot{\theta} + \tau + d_\theta, J_\phi \ddot{\phi}_d = -B_\phi \dot{\phi}_d + d_\phi \quad (14)$$

The interference terms in Eq.13 are all included in disturbances.

4.1 State Equations of Multi-sensor

First of all, we define system states x as

$$x = (\dot{\theta} \quad \dot{\phi}_d \quad \theta \quad \phi_d \quad d_\theta \quad d_\phi)^T$$

$$x = \begin{pmatrix} -\frac{B_\theta}{J_\theta} & 0 & 0 & 0 & \frac{1}{J_\theta} & 0 \\ 0 & -\frac{B_\phi}{J_\phi} & 0 & 0 & 0 & \frac{1}{J_\phi} \\ 1 & 0 & 0 & 0 & 0 & 0 \\ 0 & 1 & 0 & 0 & 0 & 0 \\ 0 & 0 & 0 & 0 & 0 & 0 \\ 0 & 0 & 0 & 0 & 0 & 0 \end{pmatrix} x + \begin{pmatrix} \frac{1}{J_\theta} \\ 0 \\ 0 \\ 0 \\ 0 \\ 0 \end{pmatrix} u \quad (15)$$

$$y = \begin{pmatrix} \dot{\phi}_d \\ \theta \\ a_x \end{pmatrix} = \begin{pmatrix} 0 & 1 & 0 & 0 & 0 & 0 \\ 0 & 0 & 1 & 0 & 0 & 0 \\ 0 & -\frac{r B_\theta}{J_\theta} & g & 0 & 0 & \frac{r}{J_\theta} \end{pmatrix} x + \begin{pmatrix} 0 \\ 0 \\ \frac{r}{J_\theta} \end{pmatrix} u$$

4.2 Design of Observer Gain

The observer gain is designed by using Kalman Filter, which is widely known as the observer for systems with white noise w , v .

$$\dot{x} = Ax + Bu + w$$

$$y = Cx + Du + v$$

$$w = \begin{pmatrix} w_{\dot{\theta}} & w_{\dot{\phi}_d} & w_{\theta} & w_{\phi_d} & w_{d\theta} & w_{d\phi} \end{pmatrix}^T \quad (16)$$

$$v = \begin{pmatrix} v_{gyro} & v_{encoder} & v_{acc} \end{pmatrix}^T$$

Here by choosing the values of system noise w and sensor noise v , better state observer can be obtained. It is necessary to set big values for system noise of disturbance w_d , w_d . Other values can be decided by specific objective. For example, when we want smooth $\hat{\theta}$, we can set the value of system noise w smaller while value of corresponding sensor noise v_{acc} bigger.

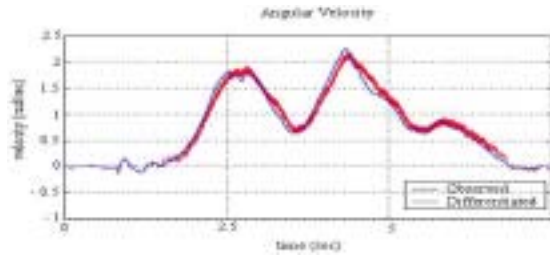


Fig.8 Estimated angular velocity (solid line: observer estimation, dashed line: differentiation of encoder outputs)

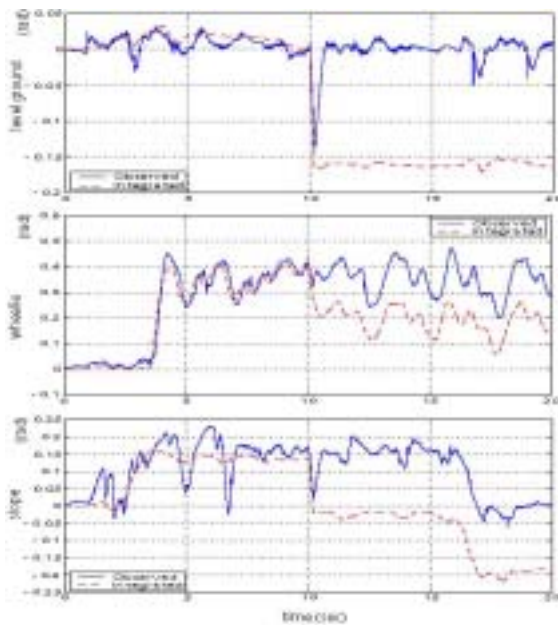


Fig.9 Estimated inclination angle (solid line: observer estimation, dashed line: integration of gyroscope output)

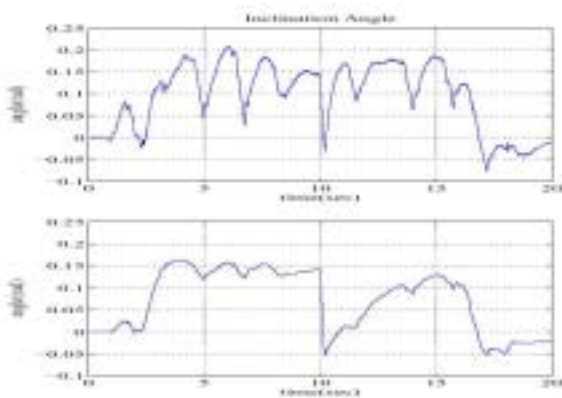


Fig.10 Different estimation by different observer gains

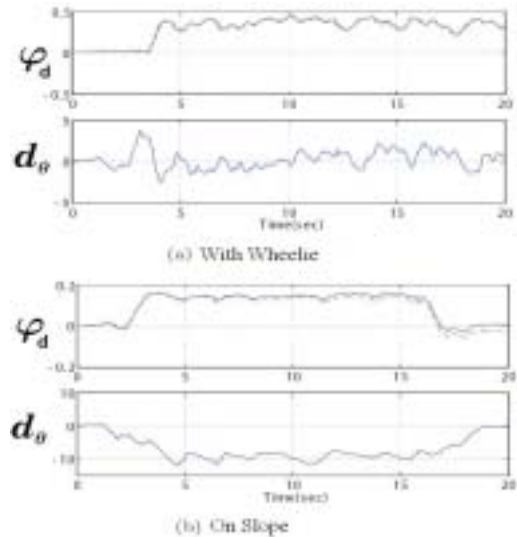


Fig.11 Distinction between a wheelie action and slope using d

From Fig.8, we can see that estimated angular velocity is earlier and smoother. In Fig.9, the upper figure shows the estimated angle of the experiment carried out on horizontal plane, the middle one shows experiment with wheelie, and the lower figure shows experiment on slope. And to test the robustness of observer, we add a disturbance at $t=10s$. It is clear that the observer is quite robust and can work well even with strong disturbance.

The estimated inclination angle depends on both gyroscope and acceleration. And the degrees of dependence can be determined by changing values in w , v . However, when degree of dependence on acceleration is higher, estimated angle will vibrate greatly because acceleration itself is in a vibrating manner. Fig.10 shows such phenomenon. And Fig.11 shows that by using this observer, it is easy to make a separation that whether wheelchair is on slope or wheelie.

5. Experiment

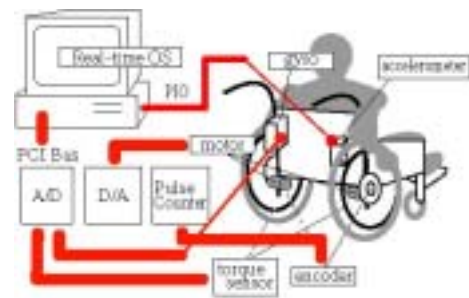


Fig.12 Experimental Setup

As shown in Fig.12, in this system there are 5 sensors for: rotating speed (ω) of the wheelchair frame, vertical and horizontal accelerations (A_{nv} , A_{ny}), angle of both wheels (θ_r , θ_l).

Experiments on horizontal plane have been carried out and the limit of torque is calculated. During the experiment, if human and motor

torque is bigger than this limit, motor output decreases so that the total torque is equal to the limit. Data are shown in Fig.13,14.

It is obvious that θ vibrates around θ_0 , but it never exceed 0. Similarly, X_{ZMP} does not cross over 0, it can be said that there is no wheelie during the experiment.

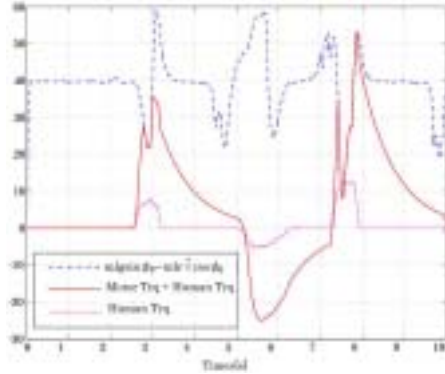


Fig.13 Experiment Data

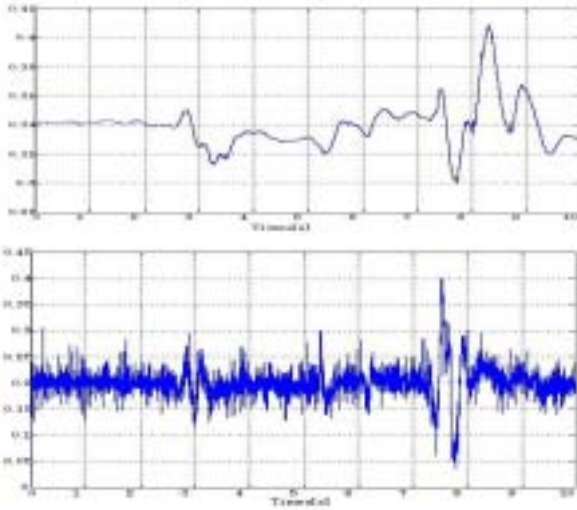


Fig.14 Observed and Calculated X_{ZMP}

6. Lagrange's Equation of System on Slope

It is on upslope, that wheelchair is easy-to-overtum. So we deduce the Lagrange's Equation of System on slope, and try to find universal criteria, which can be used both on horizontal plane and slope.

Now it will be proven that no matter how the coordination system of COM is defined the result will not be affected. As shown in Fig.15, here we define the coordination system of COM as vertical and horizontal, the velocity of COM can be calculated as below.

$$\begin{cases} v_{mx} = \frac{d}{dt}(x \cos \zeta + l \sin(\varphi - \zeta)) = \dot{x} \cos \zeta + l \cos(\varphi - \zeta) \dot{\varphi} \\ v_{my} = \frac{d}{dt}(x \sin \zeta + l \cos(\varphi - \zeta)) = \dot{x} \sin \zeta - l \sin(\varphi - \zeta) \dot{\varphi} \end{cases} \quad (17)$$

So the velocity of COM is

$$\begin{aligned} v_G^2 &= v_{mx}^2 + v_{my}^2 \\ &= \dot{x}^2 + l^2 \dot{\varphi}^2 + 2\dot{x}l\dot{\varphi}(\cos \zeta \cos(\varphi - \zeta) - \sin \zeta \sin(\varphi - \zeta)) \\ &= \dot{x}^2 + l^2 \dot{\varphi}^2 + 2\dot{x}l\dot{\varphi} \cos \varphi \end{aligned}$$

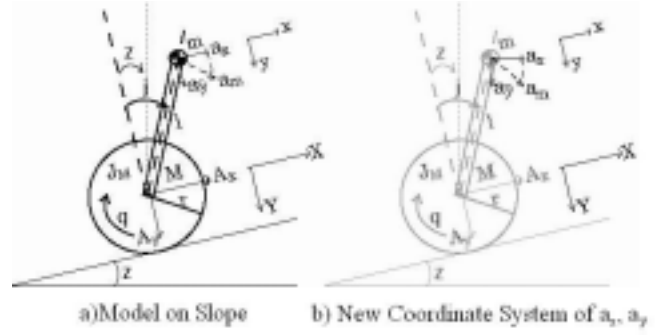


Fig.15 Coordinate System

Similarly we assume that the horizontal plane passing through the rear axle as the potential energy reference plane.

$$U = mgl \cos(\varphi - \zeta) + Mgx \sin \zeta \quad (18)$$

So the Lagrange's equation can be written as

$$\tau + d\theta = [(M + m)r^2 + J_M] \ddot{\theta} + mlr \ddot{\varphi} \cos \varphi - mlr \dot{\varphi}^2 \sin \varphi + Mgr \sin \zeta + B_M \dot{\theta} \quad (19)$$

$$-\tau + d\varphi = (J_m + ml^2) \ddot{\varphi} + mlr \dot{\theta} \cos \varphi - mgl \sin(\varphi - \zeta) + B_m \dot{\varphi}$$

Similarly to the previous section, Lagrange Criteria on slope is

$$\tau < mgl \sin(\varphi_0 - \zeta) - mlr \dot{\theta} \cos \varphi_0 \quad (20)$$

Here let $\dot{\theta} = 0$, it turns out to be the same as (Eq.13). Therefore, it can be used both on horizontal plane and slope.

7. Calculation of Gravity Vector

Theoretically, by using gravity vector, the angle of slope (ζ) can be calculated and used for preventing wheelchair from falling backward.

$$\begin{aligned} A_{ny} &= g \sin \zeta \approx g \zeta, g = \sqrt{A_{nx}^2 + A_{ny}^2} \\ \zeta &= \frac{g \zeta}{g} = \frac{A_{ny}}{\sqrt{A_{nx}^2 + A_{ny}^2}} \end{aligned} \quad (21)$$

However, there are many disturbances, and in this work main disturbances are considered as:

Forward and Backward Accelerations (Effecting on A_{ny})

Centrifugal Acceleration (Effecting on A_{ny})

Acceleration of Wheelchair Frame Rotation (Effecting on $A_{nx}, A_{ny}, r, \dot{\theta}$)

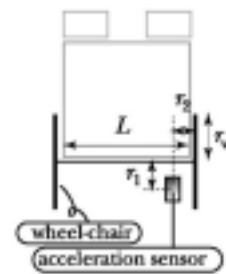


Fig.16 System View

7.1 Forward and Backward Accelerations

The forward and backward accelerations affect directly on A_{ny} . The following equation can be obtained.

$$A_{ny} = \ddot{\theta}_r r + g \zeta \quad (22)$$

7.2 Centrifugal Acceleration

The turning radius of right wheel R is defined as:

$$R = \frac{\dot{\theta}_r L}{\dot{\theta}_r - \dot{\theta}_l} \quad (23)$$

While the angle of velocity is given as the following equation.

$$\omega = \frac{\dot{\theta}_r - \dot{\theta}_l}{L} r \quad (24)$$

From above, the centrifugal force that affects A_{ny} is $r_1 \omega^2$. So the difference between acceleration of right wheel and acceleration by sensor is $r_2 \dot{\omega}$. Consequently

$$A_{ny} = g \zeta + \ddot{\theta}_r r + r_1 \omega^2 - r_2 \dot{\omega} \quad (25)$$

7.3 Acceleration of Wheelchair Frame Rotation

The centrifugal force will be generated when the wheelchair frame rotates. The force that affects A_{ny} is $r_1 \omega^2$, and that affects A_{nx} is $r_1 \dot{\psi}$.

From all of the above, the real values of A_{nx}, A_{ny} can be expressed as

$$A_{nx} = g + r_1 \dot{\psi} + D_x \quad (26)$$

$$A_{ny} = g \zeta + \ddot{\theta}_r r + r_1 \omega^2 + r_1 \dot{\psi}^2 - r_2 \dot{\omega} + D_y$$

Furthermore, the angular velocities of wheels ($\dot{\theta}_{nl}, \dot{\theta}_{nr}$) are

$$\dot{\theta}_{nr} = \dot{\theta}_r - \psi, \dot{\theta}_{nl} = \dot{\theta}_l - \psi \quad (27)$$

As stated above, the gravity vector g and angle of slope can be inferred by using the flow diagram below.

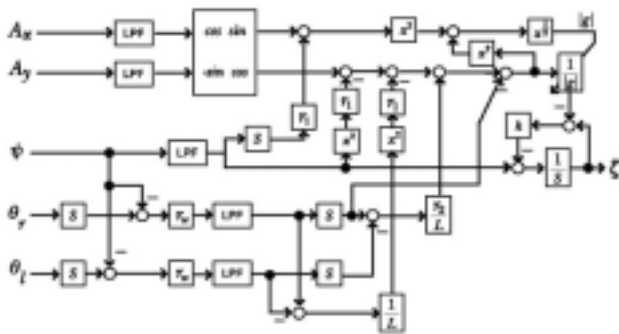


Fig.17 Data Flow Diagram

8. Experiment on Slope

In this experiment, wheelchair runs on a horizontal plane at first, and then goes to a 10° slope. The angle of slope (ζ) is calculated online using the data from sensors. As shown in the experiment data, the angle of slope can be correctly calculated. Furthermore, even if front wheels of wheelchair rise from the ground, system will not fall back because the bigger frame rotation is, the smaller torque limit will be, and without big motor output, wheelchair can easily return to its original states.

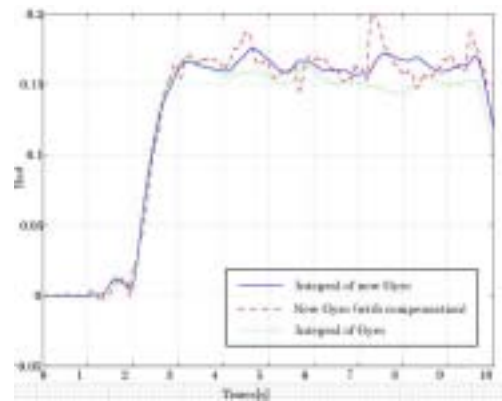


Fig.18 Inferred angle of slope

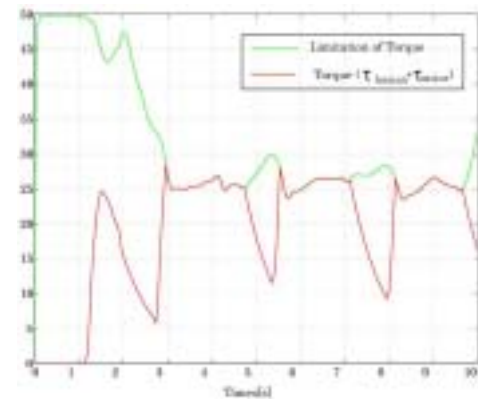


Fig.19 Experiment data

9. Conclusion and Future Work

As shown in Fig.13, at 3s and 8s, there is a sharp increase of torque. With this increase, user may feel that wheelchair accelerates on its own. To deal with this phenomenon, one simple idea is to add a low-pass filter on torque.

Also, in the experiment, mass of operator, initial angle of the vertical to COM, as well as length from rear axle to COM are treated as constants. And $m = 55\text{kg}$, $\theta_0 = 0.3415\text{rad}$, $l = 0.6\text{m}$. However, these parameters vary from person to person. So the next research theme is to find out the adequate parameters, and to accomplish the robust controller.

Furthermore, this stability condition is just the utmost limit of torque. For other control objectives, such as better ride quality and so on, other control technologies are needed.

Reference

- 1) <http://www.rehabpub.com/features/32004/5.asp>
- 2) Hata, N., Koyasu, Y., Seki, H., Hori, Y., 'Backward tumbling control for power-assisted wheelchair based on phase plane analysis, in Proceedings of the 25th Annual International Conference of the IEEE, vol.2, Sept. 2003, pp.1594-1597.
- 3) M. Vukobratovic and J. Stepaneko, 'On the stability of anthropomorphic systems, Mathematical Bioscience, 1972, vol.15, pp.1-37.
- 4) 神永拓, 0からはじめるヒューマノイドロボット第8回ロボットの歩行, ROBOCON Magazine, No.34, pp. 54-59, 2004
- 5) 梶田秀司, ゼロモーメントポイント(ZMP)と歩行制御, ロボット学会誌, Vol.20, No.3, pp.229-232, 2002